Title
CHARACTERISTICS OF AN NH3 - AIR FUEL CELL SYSTEM FOR VEHICULAR APPLICATIONS

Author
Ross, P.N.

Publication Date
1981-05-01

Lawrence Berkeley Laboratory
UNIVERSITY OF CALIFORNIA

Materials & Molecular Research Division

To be presented at the ASME 16th Intersociety Energy Conversion Engineering Conference, Atlanta, GA, August 9-14, 1981; and to be published in the Proceedings

CHARACTERISTICS OF AN NH_3 - AIR FUEL CELL SYSTEM FOR VEHICULAR APPLICATIONS

Philip N. Ross, Jr.

May 1981

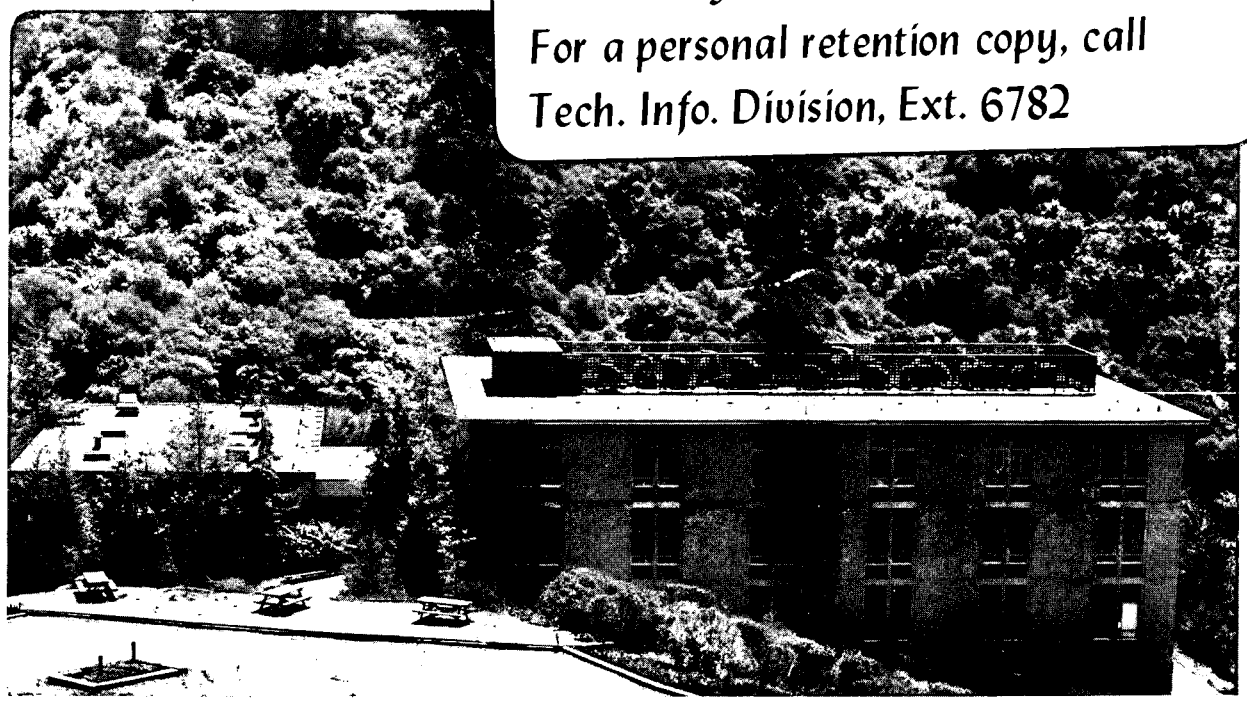

Prepared for the U.S. Department of Energy under Contract W-7405-ENG-48

DISCLAIMER

CHARACTERISTICS OF AN NH_3 - AIR FUEL CELL SYSTEM FOR VEHICULAR APPLICATIONS

Philip N. Ross, Jr.

University of California
Lawrence Berkeley Laboratory
Materials and Molecular Research Division
Berkeley, California 94720

ABSTRACT

The use of hydrogen air alkaline fuel cell in a consumer vehicle application is examined. Liquid anhydrous ammonia was found to be an excellent storage medium for hydrogen, even though the endothermicity of the NH_3 cracking reaction results in some efficiency penalty. In the system developed here, hydrogen is supplied to fuel cell by the catalytic cracking of liquid anhydrous ammonia, making the total system an indirect NH_3-air fuel cell system. The advantages of the alkaline fuel cell system relative to any acid fuel cell are higher power density (factor of 2-3) and lower cost components (factor of 2) resulting in significantly lower total cost (factor of 4-6). Laboratory scale examinations were made of the ammonia cracking reaction and the power characteristics of an alkaline fuel cell running on cracked ammonia and air. Single cell testing indicated system thermal efficiencies of 34-44% (based on H.H.V. of NH_3) can be achieved at power densities of 2600-1000 W/m^2 using currently known electrode technology. In a vehicle application, diesel ICE equivalent performance (30 W/kg) can probably be achieved using only fuel cell power with an estimated fuel cell component cost of less than $2400 (for 50 KW peak power). The primary energy consumption rate (highway cruising) is projected to be only 0.5 kWh/km with natural gas taken as the primary fuel.

INTRODUCTION

It is well known in the fuel cell field that the kinetics of oxygen reduction are more favorable in alkaline electrolyte than in acid. Materials that are poor catalysts for oxygen reduction in acid are in some cases quite good catalysts in base, e.g. Ag and Au. There is also a wider choice of inexpensive materials for use as component hardware in alkaline than in acid fuel cells. Ahlstom Atlantique[1] in particular have developed relatively inexpensive polypropylene components for a flow-type alkaline fuel cell and they project mass-production costs of $30-40 per m^2 for the bare stack (no catalysts), which is a factor of three or four lower than the projected hardware costs in phosphoric acid fuel cells[2]. The principle problem with alkaline fuel cell technology has always been the problem of hydrogen storage. In acid fuel cells, hydrogen may be stored as a liquid hydrocarbon fuel, such as methanol, and the hydrogen regenerated by steam reforming and (water-gas) shifting. The CO_2 generated from this fuel processing would cause gross insoluble carbonate formation in an alkaline electrol-

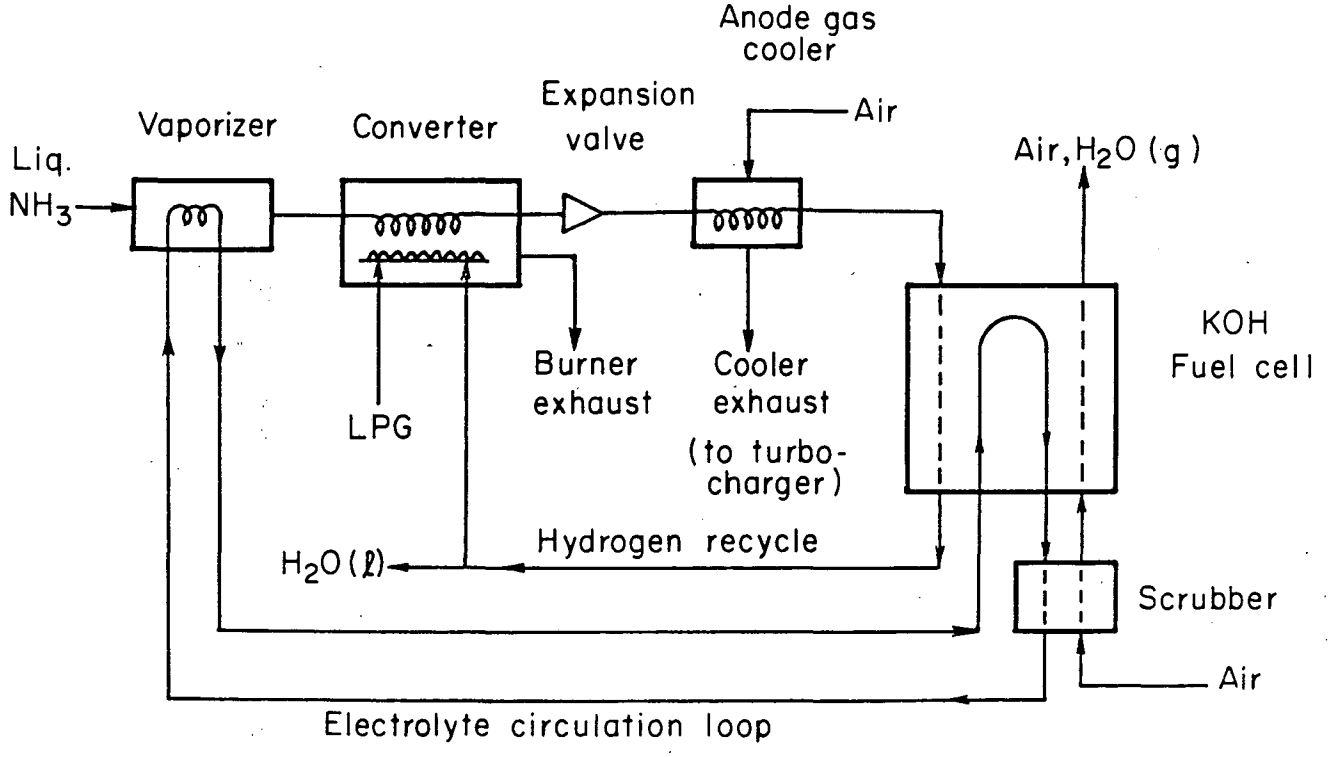

Figure 1. Flow diagram of the ammonia-air fuel cell system.

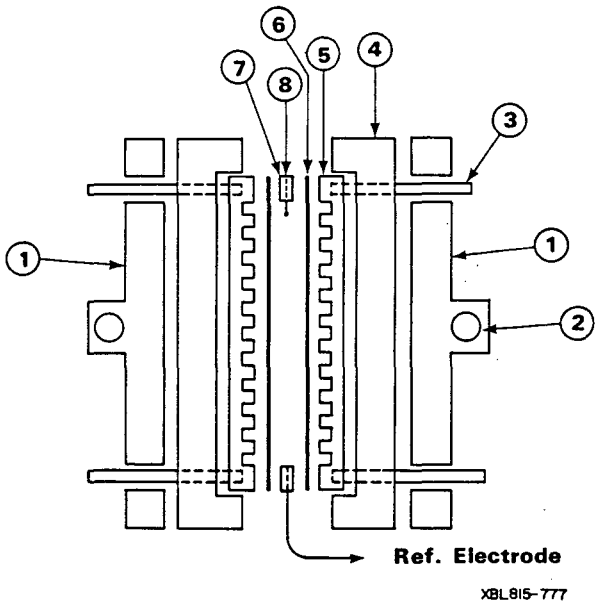

Figure 2. Schematic diagram of the laboratory hydrogen -air fuel cell (16 cm^2): 1) copper end plates; 2) cartridge heater; 3) copper tubing for carrying gas and current; 4) Teflon housing; 5) ribbed graphite plate; 6) carbon paper substrate electrodes; 7) Kel-F spacer; and 8) thermocouple.

yte, so that hydrocarbons are not appropriate storage media for hydrogen in the alkaline fuel cell. BNL[3] recently conducted a study of a hydride storage - alkaline fuel cell system for the vehicle application; but the hydride storage system was found to be much too heavy. In addition, the electrode technology used in that work was not representative of what can be achieved with modern gas diffusion electrodes, as will be shown in this work.

The objective of this study was to examine the use of anhydrous liquid ammonia as a hydrogen storage medium for a high performance hydrogen-air alkaline fuel cell. Ammonia has a higher heating value (HHV), defined by the oxidation reaction

$$2NH_3(l) + 2/3\ O_2(g) \rightarrow N_2(g) + 3H_2O(l)$$

of 21.2 kJ/g, which compares favorably with the HHV of methanol, 22.7 kJ/g. However, $NH_3(l)$ must be stored in a pressure vessel that would probably weigh more than the equivalent methanol storage vessel, so that in actual use the difference in HHV would be somewhat larger. Liquid ammonia has been proposed before as a hydrogen carrier for fuel cells[4], but detailed energy balances to determine the efficiency penalty of the endothermic generation of hydrogen from ammonia were not made. Those energy balances are made here. Also, we have made laboratory evaluations of the ammonia cracking reaction, the poisoning of Pt catalyst by unconverted ammonia, and the power density of an alkaline fuel cell using state of the art Pt electrocatalysts and electrode structures and (simulated) cracked ammonia as the anode gas. Based on these laboratory evaluations, we have developed an NH_3 - air system design for a vehicle powerplant that appears to be a very attractive alternative to other fuel cell vehicle concepts, e.g. methanol-air (acid), aluminum-air (alkaline), particularly with regard to the capital cost.

SYSTEM DESIGN

The components and material flows are shown in Figure 1. Ammonia is stored as a subcooled liquid at ca. 3 x 10^6 Pa (450 psia) at ambient temperature, is vaporized using the waste heat from the fuel cell, and fed to the converter for hydrogen generation. The converter consists of a catalytic cracker and a burner in an adiabatic box. The steady state operating condition for the converter is ca. 1 x 10^6 Pa (150 psia) and 450 C using a standard ammonia synthesis catalyst. The equilibrium conversion of ammonia to hydrogen and nitrogen can be calculated from the experimental values of the equilibrium constants tabulated by Larson and Dodge[5]. We define K_p for the reaction as written

$$2NH_3 \rightarrow N_2 + 3H_2$$

$$K_p = [P_{N_2}\ P_{H_2}{}^3/P_{NH_3}{}^2]^{\frac{1}{2}} = P\ [X_{N_2}\ X_{H_2}^3/X_{NH_3}^2]^{\frac{1}{2}} \qquad (1)$$

$$= P\ K_x \text{ or } K_x = K_p/P \qquad (2)$$

where X_i are the mole fractions and P is the total pressure. The equilibrium conversion, η, is related to K_x by

$$\eta = \sqrt{\frac{K_x}{0.918+K_x}} \qquad (3)$$

Increasing temperature increases the conversion, as the reaction as written is endothermic, and increasing pressure decreases conversion. Pressure, however, has a very favorable effect on the kinetics and on reactor volume and mass. For maximum system thermal efficiency, the converter temperature should be the minimum required to achieve conversions approaching unity; that lower limit appears to be about 450 C from the data of Larson and Dodge. At 450 C and ca. 1 x 10^6 Pa (150 psi), K_p = 151.75 (in atm.) and K_x = 15.175, so that the equilibrium conversion is 0.971. The composition of the gas leaving the cracker is, therefore, 1.5% NH_3, 24.6% N_2, 73.9% H_2. The anode gas is cooled by expansion to near ambient pressure and further air cooled to ca. 80 C, the fuel cell operating temperature. The fuel cell is of the flowing electrolyte type, with a steady-state operating condition of 80 C using 35% KOH electrolyte. Hydrogen is converted at the anode via the half-reaction

$$2H_2 + 4\ OH^- \rightarrow 4\ H_2O + 4e^-$$

Oxygen is consumed at the cathode in the half-reaction

$$O_2 + 2H_2O + 4e^- \rightarrow 4\ OH^-$$

The half-reactions clearly indicate the gradient in H_2O concentration that will develop in an operating cell. The anode gas enters the cell completely dry, and water produced in the gas diffusion electrode will probably be transported primarily by evaporation to the anode effluent and secondarily by liquid phase diffusion into the bulk electrolyte. Air for the cathode is scrubbed of CO_2 and pre-saturated with H_2O by passage through the recirculating electrolyte. Carbonate formed in the bulk electrolyte is precipitated in the coldest part of the loop, the interior of the tubing in the NH_3 vaporizer. The use of the electrolyte circulation loop to scrub CO_2 from the air is an integral part of the Al-air fuel cell design of the LLNL group[6] and appears to be an effective solution to what was once thought to be a limiting problem in alkaline fuel cells. The generation of hydrogen from ammonia is endothermic, and

requires a continuous input of enthalpy. In steady-state operation, this enthalpy is supplied (entirely) by recycling unreacted hydrogen from anode effluent gas back to the burner. During transients, such as acceleration, auxiliary heat from a small liquified propane gas cylinder is used to fine tune"load regulation" of the hydrogen supply to the fuel cell as the feedback loop would not have the correct dynamic response characteristics. LPG is also used to fire the ammonia cracker during a cold start-up.

The pressurized hydrogen gas leaving the NH_3 cracker contains excess mechanical and high quality thermal energy that can be used to drive turbines to do mechanical work, e.g. pumping the electrolyte, compression of the intake air for the fuel cell. The exact manner in which this is done has not been analyzed in detail. The excess enthalpy of reaction in the fuel cell provides the heat of vaporization for both the liquid ammonia and the product water. All product water must be vaporized to maintain an invariant electrolyte condition (weight and volume). The material and energy balance analysis, detailed in a later section, shows that the energy required in the various endothermic and parasitic processes can be met by the excess thermal energy from the exo thermic processes in the system. The total system, in fact, is a net producer of both electrical and thermal energy, the latter being a low grade waste heat at 80 C.

An important characteristic of the system observed during laboratory testing was that at ambient (ca. 20 C) temperature the cell should produce about 50% of the power produced at the steady state operating temperature of 80 C. Relative to a phosphoric acid methanol-air system, this system will be capable of cold drive-away and will not require weight penalizing heaters and insulation to come to a driving condition from a cold start.

LABORATORY STUDIES

Laboratory studies were conducted on the two major components of the system, the ammonia cracker and the hydrogen-air fuel cell. The investigation of the ammonia cracking reaction was done in conjunction with another program and the results will be published elsewhere. For this study, the objective of the experiment was to determine the size and weight of the catalyst bed necessary to achieve equilibrium conversion of ammonia at the design conditions, 450 C and 1 x 10^6 Pa (150 psi). Several commercial catalysts appeared to

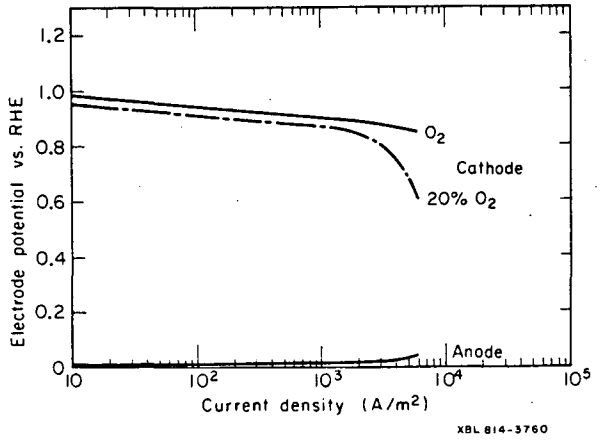

Figure 3. IR-free polarization curves for the laboratory cell with gas utilization. 35% KOH. 80 C.

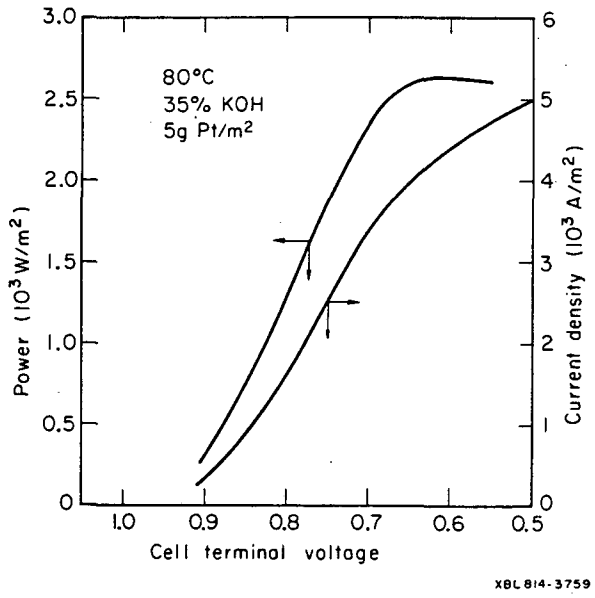

Figure 4. Power curve for the laboratory fuel cell.

work well for this application, including the least expensive like Girdler G-56, a nickel oxide on alumina, or G-41, an iron oxide on alumina. From laboratory scale (100g) reactor experience, equilibrium conversion can be achieved with ca. 15 kg of fresh G-56 catalyst at the NH_3 feed rates required for 40 KW peak power at 40% efficiency. Determination of the aging characteristics of ammonia cracking catalysts was beyond the scope of these experiments, but previous industrial experience indicates essentially no performance loss would be observed in < 5000 hr. operation. Ruthenium on alumina catalysts (Haldor-Topsoe) are significantly more active than either G-56 or G-41 and their use could reduce the catalyst weight and reactor volume by about a factor of two, but at significantly greater cost. We have not attempted to examine this tradeoff ot determine the optimum cost/weight system. The conclusion made from the laboratory studies as conducted here was that even with very inexpensive catalyst the weight and volume of the ammonia cracker is reasonable, e.g. 25 kg, 5 l.

The laboratory scale hydrogen - air fuel cell built and tested for this investigation was a single unit cell having all the components of the repeating hardware in a bipolar flowing electrolyte cellstack. A diagram of the laboratory single cell is shown in Figure 2. Because of the high current densities at which this fuel cell is intended to operate (2000-5000 A/m^2), the minimization of ohmic losses in current collection and in electrolyte resistance are essential. Backplane current collection using ribbed bipolar graphitic carbon plates as in most phosphoric acid fuel cell designs was used here for its cost effectiveness. The graphite plates were machined from solid stock (Grade ATJ, Union Carbide) and used without further treatment. The electrodes were also of the phosphoric acid fuel cell type, consisting of a polytetrafluorethylene (PTFE) bonded catalyst layer on a hydrophobic porous carbon "paper" substrate. The carbon paper (Stackpole PC 206) was wet-proofed by impregnation with PTFE, either as TFE-30B or FED 120 (DuPont), nominally 25-30 w/o PTFE solids, with a curing temperature of 350 C. The active electrode area in this cell was 16 cm^2 (4 x 4). The catalyst used in this work is a commercially available material, 10 w/o Pt supported on

Vulcan XC 72 R, purchased in this instance from Prototech. Other vendors supply a similar catalyst, e.g. Johnson-Matthey and Engelhard. We have found that the best air cathode performance is obtained by heat-treating the standard Prototech catalyst[7]. Hydrogen electrodes were fabricated from the as-received catalyst. The catalyst layers were impregnated with 25 w/o PTFE solids (DuPont TFE 30 B) and the fabricated electrode was given a final curing in air at 320 C. The interelectrode gap was maintained by a spacer machined from KEL-F® (DuPont) into which the capillary tubing from the reference electrode was fitted. The electrolyte, 35 w/o KOH, in our tests was stagnant, with the reference electrode tube acting as an additional storage reservoir. The cell housing was of solid Teflon® and the cell was "sandwiched" together using copper end plates fitted with cartridge-type heaters and a thermistor controller. No gasket was needed to seal the electrode-spacer interface.

To simulate the actual anode gas that the cell would see from the ammonia cracker, a 25% N_2 in H_2 gas mixture was passed through a saturator containing a 3.5 w/o NH_3 aqueous solution at 55 C (NH_3 vapor pressure ca. 13 kPa). The oxidant gas was a 20% O_2 in N_2 mixture that was presaturated with water vapor to match the vapor pressure of 35 w/o KOH at 80 C. The gas flow rates were adjusted and maintained using rotameters calibrated for each stream using positive displacement methods.

The polarization behavior of the fuel cell and of the individual electrodes was obtained using PAR 371 Potentiostat/Galvanostat. Single electrode potentials were measured against an external Hg/HgO reference electrode and corrected for solution resistance using current interruption by a mercury wetted relay. Polarization curves characteristic of the electrodes used in this work are shown in Figure 3. The cathode gas flow was 2.5 times the stoichiometric oxygen flow required at 5 x 10^3 A/m^2 and the anode gas flow was 1.4 times the stoichiometric flow of hydrogen required at 5 x 10^3 A/m^2. The observed dependence of the polarization on the gas flowrate indicated that nearly all the polarization at anode is due to the depletion of hydrogen from the feed gas, i.e. the electrode is operating reversibly. On pure O_2, the cathode showed perfect Tafel behavior up to 2000 A/m^2, and then some deviation from the Tafel line at the higher current densities that were flowrate dependent, i.e. utilization losses. The increased polarization on 20% O_2 relative to pure O_2 is kinetic in nature below 1000 A/m^2, but represents diffusion losses at current densities from 3000-5000 A/m^2. The diffusion losses can occur both in the gas phase (in the gas pores in the paper and catalyst layer) and in the liquid phase (the flooded agglomerates)[8]. In these particular electrodes, the diffusion losses are principally in the liquid phase. The relation of the diffusion loss to the catalyst loading is one of the critical physical limitations to increasing power density by increasing catalyst loading. The determination of the optimum catalyst loading is not a straightforward objective process, as it is highly dependent on the skill of the electrode fabricator and, in the final analysis, on the total objectives for the fuel cell component. A detailed discussion on the relation of electrode technology to total system objectives is given in a later section of the paper. The point to be made here is that using our electrode technology and a minimum fuel cell "bare stack" cost as the objective, the optimum catalyst loading is about 0.35 mg Pt/cm^2 on the cathode and 0.15 mg Pt/cm^2 on the anode using the Pt catalysts described above. Thus, the polarization curves shown in Figure 3 are representative of what we feel is the optimum electrode for this application.

The terminal cell voltage curve and the single cell power curve are shown in Figure 4. The gas flows and operating conditions are exactly the same as described for Figure 3. The interelectrode gap was 0.15 cm, representative of what could be used in full scale hardware, producing a ohmic potential drop in solution of 20 mV per 10^3 A/m^2. Since the single cell has all the components of the repeating hardware in a bipolar stack, it is reasonable to assume that the power curve for this single cell is representative of what can be achieved in a multicell stack. Further, it is the author's experience in phosphoric acid fuel cell technology that with skillful engineering and fabrication, multicell stacks of ca. 2 x 10^3 cm^2 active area closely approach the performance achieved in 25 cm^2 single cells. Therefore, it is assumed for the purposes of the analysis to be made here that the power curve of Figure 4 is characteristic of what can be achieved using contemporary electrode technology and commercially available catalysts.

Only limited endurance testing of this cell or of the electrodes themselves have been carried out. The cell was operated for a total of 10^3 hrs. using a testing profile of constant current (4500 A/m^2) for 120 hrs. at 80 C, cool to ambient at open circuit for 48 hrs., and restart. No decay ($\pm$ 10 mV) was observed in the operating characteristic of the cell between the initial start up period of ca. 100 hrs. and the end of the test at 10^3 hrs. The endurance testing of the cell was limited by other needs for the test stand and test electronics and not by the failure of the cell components. Lifetime of this particular electrode technology on the scale of 1000-3000 hrs. does not appear to be a problem. Starting up the cell after it had been cooled to room temperature indicated substantial power could be drawn from the "cold" cell, e.g. 40-50% of the maximum power at 80 C. A significant part of the power loss is due to an increase in the resistivity of the electrolyte, and it is possible that even more power could be drawn in actual use by manipulation of the caustic concentration, e.g. dilution during the cooling down period.

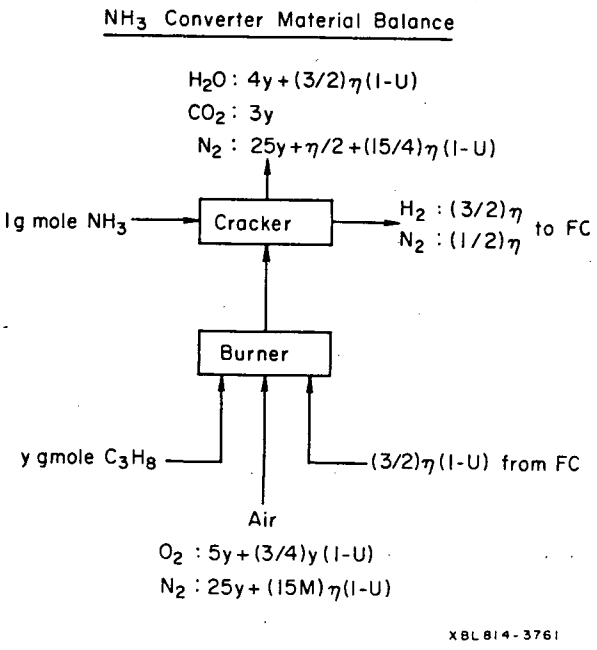

Figure 5. Material balance around the NH_3 converter subsystem.

TABLE 1

Parametric Relation of System Efficiency(ϵ) to Hydrogen Utilization (U) and LPG Consumption (y)

U	y(g mol/g mol NH_3)	ϵ
0.90	0.029	0.591V
0.85	0.021	0.583V
0.80	0.013	0.573V
0.75	0.005	0.563V
0.70	0	0.542V

XBL 814-773

SYSTEM ENERGY BALANCE

The ammonia cracking reaction is endothermic and the continuous supply of energy to the reactor necessary to sustain the reactor temperature represents a parasitic loss of efficiency of the total system. The energy balance around the cracking reactor is critical to deciding whether the total system has desireable features. The material balance around the cracker-burner subsystem is shown in Figure 5 using a 1 g mol NH_3 basis. The air flow to the burner is assumed to be the stoichiometric amount required for complete combustion of the LPG and the recycled hydrogen. U is the fraction of hydrogen fed to fuel cell that is converted to electrical energy. η is the fractional conversion of NH_3 in the cracker. y is the number of g moles of LPG required per g mole NH_3. The energy balance on the subsystem procedes as follows. We assume that the cracker-burner subsystem is adiabatic, and that the temperature of the exhaust gases equals the temperature of the hydrogen rich gas leaving the cracker (450 C). Then

$$\begin{pmatrix}\text{Sensible heat of}\\ C_3H_8+\text{air}+H_2+NH_3\end{pmatrix}+\Delta H_C=\Delta H_R+\begin{pmatrix}\text{Sensible heat of}\\ H_2O+CO_2+H_2+N_2\end{pmatrix} \quad (4)$$

where ΔH_C is the enthalpy of combustion of the LPG and H_2, and ΔH_R is the (absolute) enthalpy of the ammonia cracking reaction at 450 C. The thermochemical data required were taken from Himmelblau[8]. The resulting energy balance equation is

$$530.6y+87.11\eta(1-U)+0.48=106.4y+17.06\eta(1-U)+20.26\eta \quad (5)$$

This equation may be solved for parametric combination of y and U for a given degree of NH_3 conversion (η). The equilibrium calculations at 450 C and the laboratory studies of the NH_3 cracking reaction indicated η = 0.97 is the appropriate ammonia conversion to use for the system analysis.

Increasing the fraction of hydrogen consumed in the fuel cell increases the LPG requirement by the burner. We will show subsequently that the waste heat from the fuel cell provides sufficient energy to vaporize NH_3(l) and pre-heat the vapor to the fuel cell temperature. We can then derive a parametric relationship of the total system efficiency to the subsystem operating variables η, U, y, and v, the fuel cell voltage. We define the total system efficiency (ϵ) based on the combined HHV of NH_3 and C_3H_8 as

$$\epsilon = \frac{\text{energy produced by fuel cell}}{\text{total HHV of fuel consumed}}$$

$$= \frac{(3/2)\ \eta\ U\ (2FV)}{86.4 + 530.6\ y}$$

$$= \frac{3\eta FUV}{86.4 + 530.6\ y} \quad (6)$$

Equations (5) and (6) can be solved parametrically to give the most efficient values for the conversion of hydrogen in the fuel cell and the amount of C_3H_8 required per mole of NH_3. The result is shown in Table 1. At 70% conversion of hydrogen in the fuel cell, no C_3H_8 is required to maintain the ammonia cracking reaction. The total system efficiency is improved by consuming more of the hydrogen in the fuel cell and less in the burner, as might be expected. However, the effect is not that strong, and going to 85-90% utilization of hydrogen in the fuel cell improves the total efficiency by less than 10% e.g. at 0.7 V, the efficiency changes from 38% to 41%. For a vehicle application, changes in efficiency this small are not likely to be that important. The continuous consumption of LPG in the vehicle at 90% hydrogen utilization requires 7.6 g LPG per 100 g NH_3, so that a substantial quantity of LPG would have to be carried on the vehicle, and refueling of the vehicle would require both fuels. At this stage of evaluation of the system, it seems better to focus on the use of only NH_3 as the vehicle fuel, and use the LPG only for cold starting and for acceleration (in a vehicle powered only by a fuel cell). The total system efficiency will therefore be given by the last entry in Table 1,

$$\epsilon = 0.542\ V \quad (7)$$

The system design calls for use of the waste heat from the fuel cell, as the sensible heat in the electrolyte, to vaporize and preheat the liquid ammonia. The energy requirements for vaporization are easily determined from the T-S diagram for NH_3[9]. The maximum temperature available in the electrolyte is 80 C. We assume a ΔT of 15 C to give reasonable heat exchange area. The maximum vaporization temperature is therefore 65 C. The subcooled liquid at 20 C (or whatever the ambinet temperature) is heated to 65 C to form the saturated liquid at 2 x 10^6 Pa (450 psia), evaporated isothermally at 65 C to form saturated vapor, expanded isenthalpically to form superheated vapor at 7 x 10^5 Pa (150 psia) and 24 C, then further superheated to 65 C. The total enthalpy requirement for this process is 22.3 kJ/g mol. (5.33 kcal/g mol). The waste heat available from the fuel cell far exceeds this requirement.

The net waste heat produced by the fuel cell is the difference between the excess enthalpy of reaction and the heat of vaporization of all the product water. The excess enthalpy depends on the operating voltage of the cell (the faradaic efficiency). For a hydrogen utilization of 70%, and for cell voltages in the practical range of 0.6-0.8V, the excess enthalpy is 92-142 kJ per g-mole NH_3 feed. The heat of vaporization of the product water at 80 C is 41.5 kJ per g-mole NH_3 feed so the range of net waste heat produced by the fuel cell would be 50-90 kJ per g-mole NH_3, about 2-4 times that required for the NH_3 vaporization process.

The total system energy balance is summarized in Table 2. The left-hand column lists the endothermic processes in the system and in the right-hand column opposite the exothermic process between which heat exchange is both thermodynamically spontaneous and practical. It is clear that the system produces both electrical energy and net thermal energy at reasonable and practical operating voltages for the fuel cell.

SYSTEM CHARACTERIZATION IN THE VEHICLE APPLICATION

Actual vehicle simulation was beyond the scope of this analysis, as we really do not know enough about the weight and volume of the system at this point in

Table 2. Energy Balance Summary

(per g-mole NH_3)

Endothermic processes		Exothermic processes	
Heat of NH_3 cracking	53.30 kJ	Heat of combustion recycle hydrogen	108.7 kJ[a]
Heat of the reactants	22.95 kJ		
Heat of vaporization of NH_3	22.86 kJ	Excess enthalpy of reaction (in FC)	92-142 kJ[b]
Heat of vaporization of H_2O	41.47 kJ		
Mechanical work	N.A.	Sensible heat of anode gas	21.8 kJ

Net electrical energy = 121-162 kJ[b]

[a] 70% hydrogen utilization in the fuel cell

[b] for fuel cell voltages of 0.6-0.8 V

time. Rather, the purpose here is to make a quantitative estimate of the size and cost of the fuel cell (the electrochemical part of the system) required for this application, and then, in a more qualitative way, estimate the weight, cost and fuel consumption performance of the total system. Two different types of vehicles are considered in this analysis, the first a fuel cell/battery hybrid like that under consideration with the phosphoric acid fuel cell[10], the second a vehicle powered exclusively by the fuel cell. The hybrid vehicle is the low capital cost system, in that the fuel cell operates at a constant load near the maximum power point and the battery provides all the peaking (accelerating) power. The fuel cell only vehicle is the low operating cost system, in that the fuel cell operates at a fraction of the peak or rated power most of the time and is converting fuel much more efficiently than in the hybrid case. Using the power curve in Figure 4 and the efficiency relation of equation (7), the size of the cell stack required to produce 14 KW of rated power can be computed as a function of the total system efficiency. The results are summarized in Table 3. 14 KW rated power is the figure frequently used for the fuel cell in the hybrid powerplant as it represents the power necessary to sustain highway speeds for a typical passenger vehicle[10]. If we compare the size of the fuel in this system to that of the phosphoric acid fuel cell in the methanol-air system[11], at a comparable overall fuel efficiency of ca. 38%, the alkaline cell requires only one-third the electrode area and one-fifth the total Pt loading due to the superior power density of the alkaline cell.

The projected cost of fuel cell stacks is, of course, a difficult issue at best. The cost projection we make here is based on the current producer price of Pt, $15 per gram, and the manufacturing cost of the cell hardware projected by Ahlstom Atlantique for alkaline cells of the type in this design, $54 per m^2 ($5 per ft^2). The cost equation we use is

$$SC = [HC + (CC)\,L]\,A \qquad (8)$$

where SC is the stack cost, HC is the hardware and manufacturing cost, CC is the catalyst cost, L the catalyst loading, and A is the total cell area required to

TABLE 3

14 KW ALKALINE FUEL CELL

ϵ^b	V^a	P (W/m^2)	A (m^2)	Pt cost	Stack cost
33.5	0.619	2630	5.3	398	684
36.2	0.667	2550	5.5	413	710
38.7	0.714	2230	6.3	473	813
41.2	0.761	1750	8.0	600	1032
43.9	0.810	1015	13.8	1035	1780

[a] 97% conversion of NH_3 in perfectly adiabatic reactor, 70% utilization of hydrogen in cell.

[b] Based on H.H.V. of NH_3

XBL814-3762

achieve the rated power at the rated efficiency. The cell area in turn depends on the catalyst loading and the catalyst activity by the relation

$$A = \frac{RP}{P}\,,\quad P \propto L \qquad (9)$$

where RP is the rated power for the cell and P is the power density which has a functional dependence on catalyst loading. The functional dependence is highly non-linear, e.g. about 0.5 order in the Pt loading for our electrodes. Combining (8) and (9)

$$SC = \frac{(HC)(RP)}{P} + \frac{(CC)(L)(RP)}{P}$$

$$SC \simeq \frac{C_1}{L^{0.5}} + C_2\,L^{0.5} \qquad (10)$$

where C_1 and C_2 are constants that reflects hardware cost and catalyst costs respectively. The relation in (10) between SC and L clearly has a minimum corresponding to the optimum catalyst loading (for a particular catalyst and at fixed fuel cell efficiency). When $C_1 < C_2$, the optimum loading will clearly be lower than when $C_1 < C_2$, i.e. with relatively inexpensive hardware, the optimum loading is lower than with relatively expensive hardware. The alkaline fuel appears to have a lower projected hardware cost than the phosphoric acid fuel cell[12], so it would be expected that the optimum Pt loading (the same catalyst) would be at a lower absolute value for the alkaline cell than for the acid cell. This seems to be the practical result as well, as the optimum we find here for the low cost hardware ($54 m^{-2}) is about 0.5 mg Pt/cm^2 whereas in the phosphoric acid cell (at comparable system efficiency) the optimum loading is typically 1.0 mg Pt/cm^2 for hardware costs projected to be $130 m^{-2} [12]. The total projected cost of the 14KW alkaline fuel cell operating in an NH_3-air system at ca. 38% fuel efficiency is less than one-fifth (!) the projected cost of the 14KW phosphoric acid fuel cell operating in methanol-air system at ca. 38% fuel efficiency[12].

In the analysis of fuel cell systems, the emphasis is frequently on the thermal efficiency; that is, we calculate the size of the system required to deliver energy at a given efficiency, as done here. In the vehicle application, it is perhaps more meaningful to express the efficiency of the system in terms of the net energy delivered by the system per unit weight of fuel consumed. Then assuming various vehicle weights, one can easily estimate the fuel consumption rate and the weight of fuel required for normal range. These quantities are summarized in Table 4. The fuel consumption rates were derived using a 78% power train effi-

TABLE 4

NH_3 Consumption Rate* for a 14 kW Alkaline Cell in a FC/Battery Hybrid Vehicle

V	Size (m^2)	Cost	kcal/gNH_3	km/kgNH_3 1.0	1.25	1.50	1.75T
0.619	5.3	684	1.70	15.4	12.3	10.3	8.8
0.667	5.5	710	1.83	16.5	13.2	11.0	9.4
0.714	6.3	813	1.96	17.7	14.2	11.8	10.1
0.761	8.0	1032	2.09	18.9	15.1	12.6	10.8
0.810	13.8	1780	2.23	20.2	16.2	13.5	11.5

*highway cruising at constant speed

XBL815-776

ciency assuming the energy required for sustained cruising is 100 WH/T km[13] (where T is in tonnes). For qualitative comparison, the methanol-air fuel cell/battery hybrid vehicle of similar design (1.56T) has a projected methanol consumption rate of ca. 13 km/kg in an urban driving cycle and about 10-11 km/kg on highway cruising with the fuel cell operating at 38% thermal efficiency[11]. The appropriate figure for the comparable NH_3-air hybrid vehicle is the entry for a cell voltage of 0.714 and 1.5-1.6 metric ton vehicle, 10-12 km/kg. Both vehicles have comparable projected fuel consumption rates but the NH_3-air vehicle has far superior capital cost, $813 vs. ca. $3000, due to the superior power density of the alkaline cell at comparable efficiencies.

The second type of vehicle to be treated here is a fuel cell only powered vehicle, analogous to the aluminum-air fuel cell powered vehicle. Such a vehicle would have the ultimate in fuel consumption rate, since the power required for cruising is only one-third the peak power and the efficiency will be much higher than in the hybrid vehicle where the fuel cell is always operated close to peak power. The cost of the fuel cell component will be approximately three times that for the hybrid powerplant, or about $2000 according to the cost projections made here. However, the fuel consumption rate will be about one-half the rate of the hybrid vehicle. From an economic standpoint, the critical factor is likely to be the life-cycle cost, the sum of the capital cost and the operating cost over the life of the vehicle. Such a life-cycle cost analysis is clearly beyond the scope of the present investigation. We outline here only the projected capital cost and fuel consumption rate which can be used for comparison to other systems. The vehicle is taken to have characteristics of diesel ICE powered vehicle, which means 30 W/kg mechanical peak power, or 33.3 W/kg fuel cell peak power for an electric motor efficiency of 90%. The fuel cell was sized to give the required peak power using the power curve (Figure 4), with vehicle total weight as a parameter. The fuel consumption rate for sustained cruising at highway speed was calculated assuming 78% power train efficiency and that 14 KW are required at 100 WH/T km. The results are summarized in the final Table. Unlike the fuel cell/battery hybrid vehicle, the fuel cell powered vehicle would not necessarily have improved fuel consumption rate in urban driving due to the loss of efficiency during acceleration periods. Even if the hybrid vehicle gets 10-20% better consumption rate in urban driving, the fuel cell powered vehicle would still have a superior fuel consumption rate on an integrated driving profile, provided both vehicles had equal total weights. The projected gasoline equivalent mileage for the NH_3-air system in a GM X-car type of vehicle (ca. 1.5 metric tons) would be 52 mpg, far superior to the mileage obtained in a diesel ICE powered X-car.

Quantitative comparison of the NH_3-air fuel cell concept with the aluminum-air fuel cell requires the reference of both systems back to a common primary fuel to compare system efficiencies. The most reliable reference points are obtained by using coal as the primary energy source for aluminum, and natural gas as the energy source for ammonia. According to the LLNL evaluation of aluminum-air vehicles[14], the primary energy consumption rate is projected to be 1.47-1.93 kWh/km for the equivalent vehicle considered here. The net energy consumed to produce anhydrous liquid ammonia is 7.82×10^{-3} kWh/g NH_3. Using the fuel consumption rate for the 1.5 tonne X-car type vehicle (with 30 W/kg) in Table 5, the NH_3-air powerplant has a projected primary energy consumption rate of 0.52 kWh/km.

Little of anything has been said about the weight of the NH_3-air fuel cell system, and the preceeding discussion has been based entirely on the assumption that vehicles of equal weights and power to weight ratios (PWR) could be developed. An analysis of weight is difficult for a system which is as undeveloped as this one. Using polypropylene and graphite as the cell hardware with a 0.15 cm interelectrode gap, the wet

TABLE 5

FC Cost and NH_3 Consumption Rate for a NH_3-Air FC Powered Vehicle

Vehicle Gross Wgt. (metric tons)	FCPP (kW)	Size (m^2)	Cost ($)	NH_3 Rate* (km/kg)
1.0	33.3	12.3	1587	20.2
1.25	41.6	15.4	1987	16.7
1.5	50.0	18.5	2387	14.1
1.75	58.3	21.6	2786	12.3

XBL814-775

* highway cruising at constant speed

cell weight would be ca. 160 kg for 50 KW FCPP. The ammonia cracking-burner unit would be ca. 40 kg based on the use of Girdler G-56 catalyst. The ammonia fuel tank, vaporizer, heat exchangers, condenses, pumps, and electrolyte loop are estimated to be an additional 100 kg making the total weight 300 kg. The ammonia weight for 500 km range is about 36 kg. The weight of the vehicle body, drivetrain and motor-controller is taken to be that for the aluminum-air vehicle minus the battery, 890 kg. Adding 136 kg for passengers gives a total gross weight of 1360 kg which is within the 1.5 tonne weight used to estimate the fuel consumption rates.

CONCLUSIONS

Based on the laboratory studies of NH_3 cracking and alkaline H_2-air single cells, an indirect NH_3-air alkaline fuel cell system appears to have excellent power and cost characteristics for application as a vehicle power source. In hybrid fuel cell/battery concept, a 14 KW fuel cell system could be fabricated from existing technology that would have a thermal efficiency of 38-44% at power densities of 1000-2200 W/m^2 with fuel cell component costs of $800-1800 depending on the efficiency desired. This is about 25-30% of the cost of the 14 KW phosphoric acid fuel cell component that can be built with existing technology. The power density (by weight and volume) of the total NH_3-air system appear to be high enough to consider use in a fuel cell only powered vehicle. A passenger vehicle gross weight of 1.5 tonnes with mechanical peak power of 30 W/kg appears possible. The 50 KW peak power alkaline cell would cost ca. $2400 and on highway driving at steady speed obtain 14.1 km/kg NH_3, which corresponds to a primary energy consumption rate of only 0.52 kWh/km (natural gas as primary fuels).

REFERENCES

1. Dr. B. Waszawski, Alsthom Atlantique, personal communication, March 1981.

2. A. J. Appleby and F. Kalhammer, "The Fuel Cell: A Practical Power Source for Automotive Application", Drive Electric 80, Wembly, London, England, October 14-17, 1980.

3. Brookhaven National Laboratory Contract No. 534582-S (1979); also, D. Lynn, Los Alamos National Laboratory Report LA-UR-80-3094 (1980).

4. Escher: Foster Technology Associates, Report to BNL 51210 (1980).

5. A. Larson and R. Dodge, J. Am. Chem. Soc., 45, 2918 (1923).

6. J. Cooper, R. Homsy and J. Landrum, "The Aluminum-air Battery for Electric Vehicle Propalsion", in Proc. 15th I.E.C.E.C., Seattle, WA., August 18-22, 1980.

7. P. N. Ross, Jr., Electric Power Research Institute Report EM-1553, September 1980.

8. D. Himmelblan, "Basic Principles and Calculations in Chemical Engineering", Prentice-Hall, Third Edition 1974, pp 493-504.

9. O. Hougen, K. Watson and R. Ragatz, "Chemical Process Principles, Part II", J. Wiley, 1947, pg. 631.

10. B. McCormick, J. Huff, S. Srinivasan, and R. Bobbett, "Applications Scenario for Fuel Cells in Transportation", LASNL Report LA-7634-MS (February 1979).

11. D. Lynn, B. McCormick, R. Bobbett, S. Srinivasan and J. Huff, Proc. 16th I.E.C.E.C., Atlanta, GA., August 9-14, 1981.

12. See ref. 2. Also personal communication from A. J. Appleby, EPRI, March 1981.

13. Provided by E. Behrin, Lawrence Livermore National Laboratory, March 1981.

14. J. Cooper, "Estimates of the Cost and Energy Consumption of Aluminum-air Electric Vehicles", LLNL Report UCRL-84445.

ACKNOWLEDGEMENTS

This work was supported by the Assistant Secretary of Conservation and Renewable Energy, Office of Advanced Conservation Technology, Electrochemical Systems Research Division of the USDOE under contract number W-7405-ENG-48.

TECHNICAL INFORMATION DEPARTMENT
LAWRENCE BERKELEY LABORATORY
UNIVERSITY OF CALIFORNIA
BERKELEY, CALIFORNIA 94720